RESEARCH ARTICLE

Guofeng MA, Renke KANG, Zhigang DONG, Sen YIN, Yan BAO, Dongming GUO

Hole quality in longitudinal–torsional coupled ultrasonic vibration assisted drilling of carbon fiber reinforced plastics

Abstract Carbon fiber reinforced plastic (CFRP) composites are extremely attractive in the manufacturing of structural and functional components in the aircraft manufacturing field due to their outstanding properties, such as good fatigue resistance, high specific stiffness/strength, and good shock absorption. However, because of their inherent anisotropy, low interlamination strength, and abrasive characteristics, CFRP composites are considered difficult-to-cut materials and are prone to generating serious hole defects, such as delamination, tearing, and burrs. The advanced longitudinal–torsional coupled ultrasonic vibration assisted drilling (LTC-UAD) method has a potential application for drilling CFRP composites. At present, LTC-UAD is mainly adopted for drilling metal materials and rarely for CFRP. Therefore, this study analyzes the kinematic characteristics and the influence of feed rate on the drilling performance of LTC-UAD. Experimental results indicate that LTC-UAD can reduce the thrust force by 39% compared to conventional drilling. Furthermore, LTC-UAD can decrease the delamination and burr factors and improve the surface quality of the hole wall. Thus, LTC-UAD is an applicable process method for drilling components made with CFRP composites.

Keywords longitudinal–torsional coupled, ultrasonically drilling, CFRP, thrust force, hole quality

1 Introduction

With the increasing requirement of high-strength and lightweight materials in the aircraft manufacturing field, carbon fiber reinforced plastic (CFRP) composites have been widely applied in the manufacturing of structural and functional components because of their good fatigue resistance, high specific stiffness/strength, good shock absorption, and other characteristics [1–3]. For instance, approximately 50% of the main structural components of Boeing 787 are made of CFRP composites [4]. In aircraft manufacturing processes, composite components can realize near-net shape manufacturing [5]. However, millions of holes must be machined on them for bolt and rivet connections to facilitate their assembly [6,7]. Thus, CFRP drilling is indispensable, and the hole quality directly affects the assembly quality of aircrafts. However, the machinability of CFRP composites under the drilling is extremely poor because of their inherent anisotropy, low interlamination strength, and abrasive characteristics [8–11]. Under the action of axial cutting force, serious defects, such as delamination, tearing, burrs, and glass transition of resin, are easily generated. Among them, delamination is the primary threat because it deteriorates the mechanical and fatigue strengths of the materials around the holes. In addition, carbon fiber with high hardness has a severe pressing and friction effect on the cutting edge and flank surface of drills, resulting in shortened drill bit life.

Ultrasonic vibration assisted drilling (UAD) is a compound machining method that combines ultrasonic vibration assisted machining technology and conventional drilling (CD) to improve the performance of drilling difficult-to-cut materials [12]. In the UAD process, the mechanical vibration with ultrasonic frequency is imposed on the drill, changing the contact state between the cutting edge and the workpiece from continuous contact to discontinuous contact. The thrust force, torque, and drilling temperature can be reduced by the micro-impact of the cutting edge on the material, the improved lubrication, and the reduced friction coefficient between the cutting edge and the workpiece. Consequently, superior drilling quality with less defects and low hole wall surface roughness can be obtained [13–16].

In the existing research on the UAD of CFRP

Guofeng MA, Renke KANG, Zhigang DONG (✉), Sen YIN, Yan BAO, Dongming GUO
Key Laboratory for Precision and Non-Traditional Machining of Ministry of Education, Dalian University of Technology, Dalian 116024, China
E-mail: dongzg@dlut.edu.cn

composites, longitudinal UAD (L-UAD) technology is mainly used. Searches yield many studies related to hole quality in the L-UAD of CFRP composites. Makhdum et al. [17] compared the drilling performance of UAD and CD and concluded that UAD generates reduced cutting force and torque, good surface quality and improved roundness, and low delamination factor but high cutting temperature. Furthermore, the authors speculated that UAD promotes the brittle-to-ductile transition in CFRP. Sanda et al. [18] studied the drilling thrust force, temperature, delamination, burrs, and surface quality in the UAD of CFRP composites and Ti6Al4V. They reported that each spindle speed has an optimal feed rate that maximizes the impact of ultrasonic vibration. Moreover, UAD performs better than CD.

Many studies [19–21] have proven that 2D ultrasonic vibration performs better than CD in machining difficult-to-cut materials. To improve the drilling performance, some researchers developed the longitudinal–torsional coupled UAD (LTC-UAD) by combining the 2D ultrasonic vibration and CD. LTC-UAD is a 2D-UAD technology that vibrates the drill along a 2D trajectory in the cutting plane. Amini et al. [22] researched the reduction of thrust force in the LTC-UAD of 7075-T6 aluminum alloy. They concluded that LTC-UAD could lower the thrust force significantly than CD and explained the reduction of thrust force from the perspective of the chip and tool front angle. Liu et al. [23] compared the longitudinal–torsional vibration performance of horn with helical and straight grooves through numerical simulation and experiment. Their results show that both groove types can turn the longitudinal ultrasonic vibration into LTC ultrasonic vibration, but the horn with a helical groove can obtain a larger torsional amplitude than that with a straight groove. Niu et al. [24] developed a multi-objective optimization model for process parameters in the LTC ultrasonic vibration assisted milling of titanium alloy using non-dominated sorting based algorithm II and verified the model through milling experiments. Wang et al. [25] carried out an experimental research on the thrust force in

rotary UAD (RUD) of ceramic matrix composites using LTC core drills. Their results show that the thrust force reduction of LTC-RUD can exceed 50% compared with conventional RUD. Paktinat and Amini [26] conducted a comparative research on the drilling of AISI 1045 using CD, L-UAD, and LTC-UAD, adopting finite element method and experimental method. They proved that LTC-UAD has superior characteristics over L-UAD in the aspects of thrust force, hole wall quality, drilling temperature, and drill wear.

At present, LTC ultrasonic vibration assisted machining technology is mainly used to mill and drill metal materials. The research on the LTC-UAD of CFRP composites is rare. Therefore, this research performed drilling experiments on CFRP composites using a self-developed LTC-UAD system and the L-UAD system to study the drilling performance in terms of cutting force, hole defects, and hole wall roughness.

2 Characteristics of LTC-UAD in kinematics

The schematics of CD, L-UAD, and LTC-UAD are shown in Fig. 1. The motion of CD consists of the rotary and axial feeding motions of the drill. L-UAD is formed by imposing longitudinal ultrasonic vibration on the motion of CD. In the process of LTC-UAD, as shown in Fig. 1(c), the drill is not only rotating and axial feeding, but also carrying out high-frequency vibration in the axial direction and torsional vibration in the tangential direction. Consequently, the drill makes a periodic variable motion in both axial and tangential directions.

The actual rotating angle of the drill is the sum of the rotating angle of the drill rotating with the spindle and the rotating angle generated by the torsional vibration. The rotation angle (φ_t) generated by torsional vibration in time t can be calculated as follows:

$$\varphi_t = \varphi_0 \sin(2\pi f t + \varphi'), \tag{1}$$

where φ_0 represents the angular amplitude of torsional
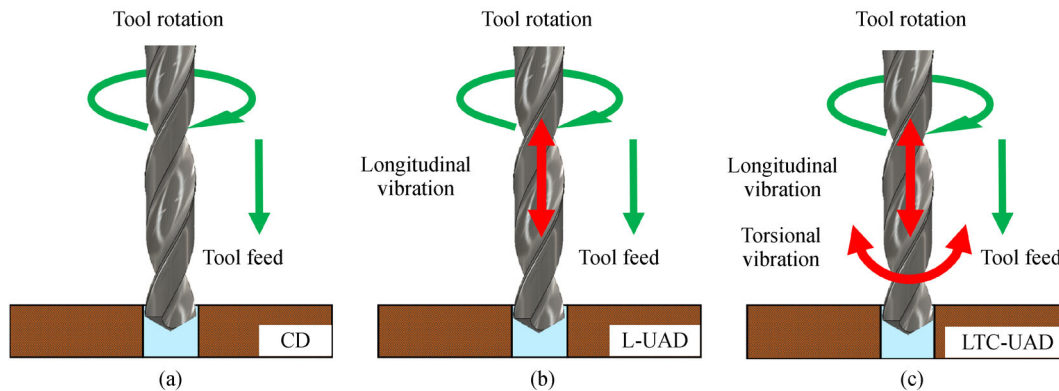

Fig. 1 Schematics of (a) CD, (b) L-UAD and (c) LTC-UAD.

vibration, f represents the ultrasonic vibration frequency, and φ' represents the phase difference between the torsional and longitudinal vibrations.

The spindle rotates at constant speed, so the actual rotation angle (φ) of the tool in time t is

$$\varphi = \omega_0 t + \varphi_t, \tag{2}$$

$$\omega_0 = 2\pi n/60, \tag{3}$$

where ω_0 represents the rotating angular velocity of the spindle, and n represents the spindle speed.

In summary, the motion trajectories of the main cutting edge in LTC-UAD are expressed as follows:

$$\begin{cases} x = R\cos\left(2\pi nt/60 + \varphi_0\sin(2\pi ft + \varphi')\right), \\ y = R\sin\left(2\pi nt/60 + \varphi_0\sin(2\pi ft + \varphi')\right), \\ z = Ft + A\sin(2\pi ft), \end{cases} \tag{4}$$

where R represents the drill radius, F represents the feed rate, and A represents the amplitude of ultrasonic vibration.

Figure 2 shows the trajectories of the optional point on the main cutting edge of the drill in CD, L-UAD, and LTC-UAD. The trajectories were plotted by MATLAB according to the corresponding trajectory equations.

3 Experimental work

3.1 Experimental setup

The experiments were carried out on a three-axis computer numerical control machining center (NHM800, Ninghua Machine Tool Co., Ltd., China). As shown in Fig. 3, the experimental setup includes the UAD and cutting force measuring units. The UAD unit is the key part of the experimental setup, which includes an ultrasonic generator, two kinds of UAD tool holder (i.e., LTC-UAD and L-UAD), and a high-speed steel (HSS) twist drill. The ultrasonic generator converts the conventional 50 Hz electrical power to an ultrasonic frequency ($\geqslant 20$ kHz) AC energy, which is transmitted to a piezoelectric transducer.
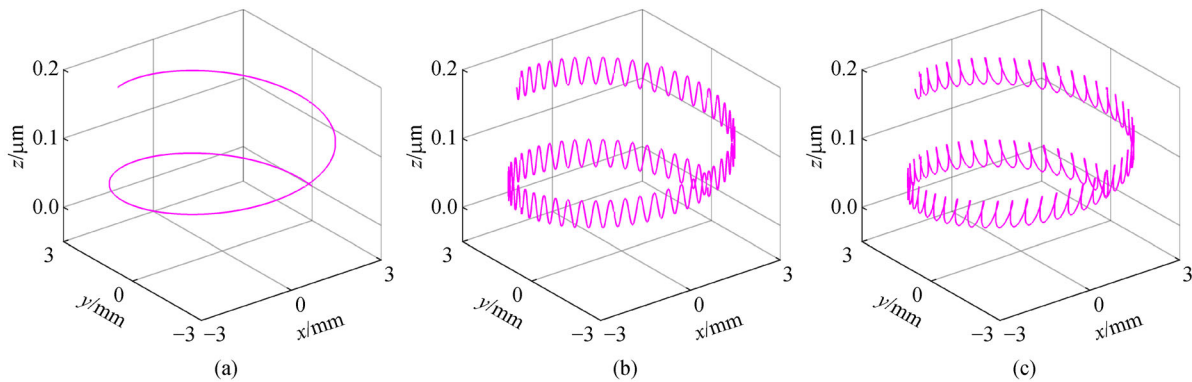

Fig. 2 Trajectories of optional point on the main cutting edge of the drill in (a) CD, (b) L-UAD, and (c) LTC-UAD.
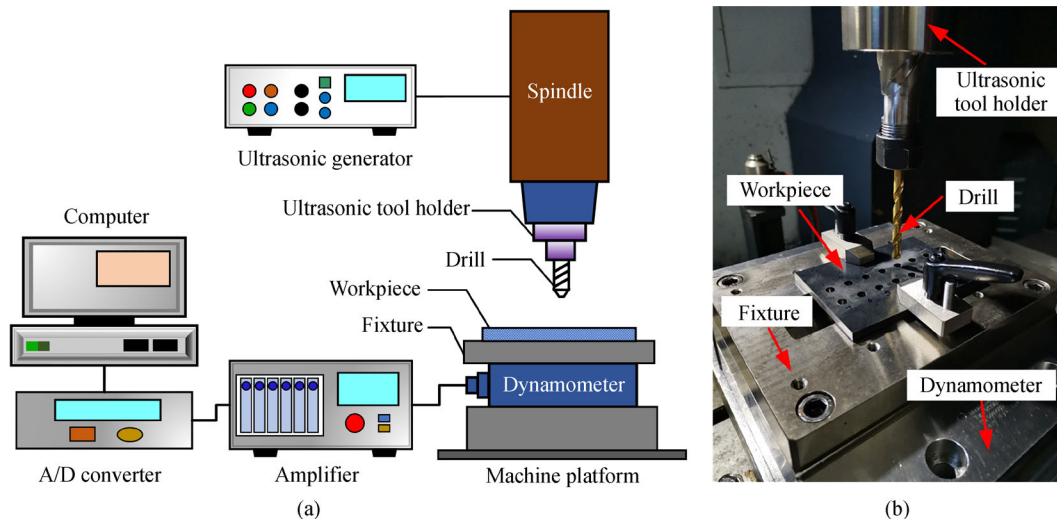

Fig. 3 Experimental (a) schematic and (b) setup of UAD.

The realization of LTC vibration is dependent on a horn with a spiral groove. As shown in Fig. 4(b), the longitudinal ultrasonic vibration produced by the transducer is amplified and converted to LTC vibration through the spiral grooves on the horn. The torsional and longitudinal vibration modes have the same resonant frequency and a phase difference. The 0.4 amplitude ratio of torsional vibration to longitudinal vibration was obtained using the transient dynamics simulation module of ABAQUS. The longitudinal amplitude of the drill can be measured by a laser displacement measurement sensor (LJ-H025, Keyence Co., Japan). Under different settings of the output control of the ultrasonic generator, the amplitude of longitudinal vibration can be adjusted from 0 to 12 μm. A standard two-flute twist drill (HSS, TiN coated, φ6 mm) with a point angle of 118° and a helix angle of 33° was used in the experiments.

3.2 Workpiece material

As shown in Fig. 5, a 5 mm thick T800 CFRP composites plate was selected as the workpiece material in the experiments, consisting of 28 plies of prepreg with a stacking sequence of $[-45/0_2/45/0/90/0]_{S2}$. The CFRP composites plate was cut into 100 mm × 75 mm pieces. The material physical properties of T800 prepreg are listed in Table 1 [27].

3.3 Measurement and evaluation

A multicomponent dynamometer (9139AA, Kistler Instrumente AG, Switzerland) was used to record the thrust forces during the experiments. The dynamometer converts cutting forces into electrical signals, which are processed by a multichannel charge amplifier (5080, Kistler Instrumente AG, Switzerland) and transformed and delivered to the computer through an analog to digital converter card (5697A1, Kistler Instrumente AG, Switzerland). The digital force signals are further processed by Dynoware and displayed on the computer screen. The measured thrust force is the average of the actual thrust forces because the sampling frequency of the dynamometer cannot keep up with the frequency of ultrasonic vibration.

The defects include delamination, tearing, and burrs. The delamination defects induced by the drilling process reduce the surface integrity of composite materials and thus affect the structural strength and stiffness of the composite components. Therefore, as shown in Fig. 6(a), the extent of delamination was evaluated by the delamination factor (F_D), which is the ratio of the diameter (D_{del}) of the circle that encompasses the delamination area to the nominal diameter (D_{nom}) of the drilled hole [28]. The 2D burr factor (F_B) shown in Fig. 6(b) was used to quantitatively evaluate the burr defects at the hole exit, which is the ratio of the area (A_{bu}) of all burrs to the
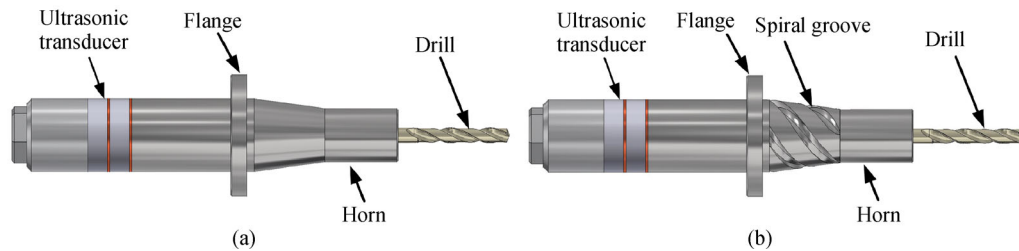

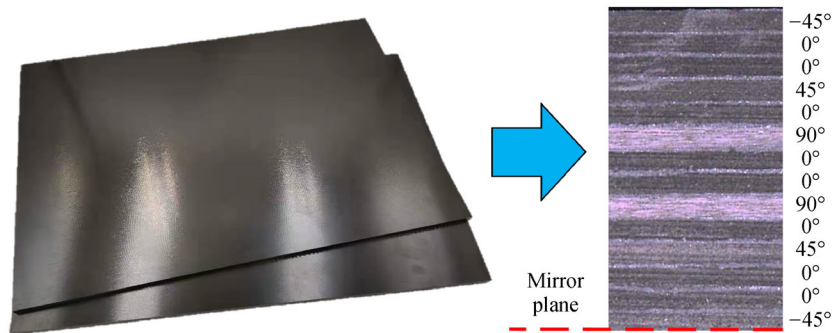**Fig. 4** (a) L-vibration unit and (b) LTC-vibration unit.

Fig. 5 CFRP composites plate.

Table 1 Material physical properties of the T800 CFRP unidirectional plate [27]

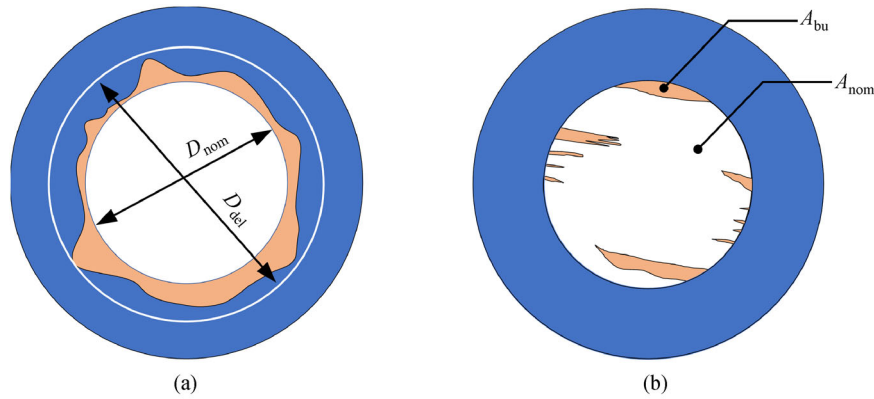| Density	Longitudinal Young's modulus	Longitudinal shear modulus	Transverse Poisson's ratio	Tensile strength	Compressive strength
2.7 g/cm^3	160 GPa	6.21 GPa	0.36	2.843 GPa	1.553 GPa

Fig. 6 Schematics of (a) delamination factor (F_D) and (b) burr factor (F_B).

nominal area (A_{nom}) of the drilled hole. The super depth of the field microscope (VHX-600E, Keyence Co., Japan) was applied to observe the hole exit morphology of the drilled hole and measure the burr diameters (D_{del}) and areas (A_{bu}) using the built-in measurement function.

$$F_D = D_{del}/D_{nom}, \quad (5)$$

$$F_B = A_{bu}/A_{nom}. \quad (6)$$

Finally, the drilled holes were cut along its axis, applying a diamond wire saw machine and the micro-morphology of the hole wall, including carbon fibers, and the resin matrix was observed with a scanning electron microscope (Q45, Fei Co., USA). The Tyler Hopson surface profiler (CLI2000, Taylor Hobson Ltd., UK) was selected to measure the surface roughness of hole wall based on contact measurement principles. The surface roughness measurements were taken on the middle of the hole wall, and the sampling length was set to 3 mm to avoid the influence of inlet and outlet defects on the values of hole wall roughness.

3.4 Experimental design

Each group of experimental parameters was applied under LTC-UAD, L-UAD, and CD conditions using the LTC-UAD and L-UAD tool holders. The CD experiments could be carried out using the L-UAD tool holder when the ultrasonic generator was turned off. The spindle speed was set to 2000 r/min for all of the drilling experiments. The feed rate was set to 0.005, 0.01, 0.015, and 0.02 mm/r. The single factor method was adopted in the experiments. All machining parameters used in the drilling procedures are

listed in Table 2. To ensure the repeatability of the experimental results, each group of experiments was repeated thrice. One drill was used to machine only one hole to avoid the effect of tool wear on the experimental results.

4 Results and discussion

4.1 Thrust forces

The thrust forces imposed on the workpiece by the cutting edge were recorded for CD, L-UAD, and LTC-UAD. The typical variation curves of the thrust forces with the cutting time under three conditions are shown in Fig. 7. The variation process of thrust force generally consists of three stages. In the stage of entering, the contact length between the workpiece and the main cutting edge increases with the feeding of the drill. Consequently, the thrust force increases gradually until the maximum value is reached. In the stage of stable drilling, the main cutting edge of the drill has completely penetrated the material, and the drill continues moving forward. The fluctuation of thrust force is relatively stable, and the maximum value of thrust force is obtained at this stage. At the end of the stable drilling stage, the supporting stiffness of the hole bottom material gradually weakens as the thickness of the uncut layers below the drill gradually decreases with the advance of the drill, and the material deforms under the thrust force induced by the drill. Therefore, the thrust force presents a steady downward trend. When the drill tip reaches the exit region of the hole, that is, in the stage of exiting, the drill begins to drill through the material, and the contact length between the workpiece and the main cutting edge

Table 2 Experimental parameters

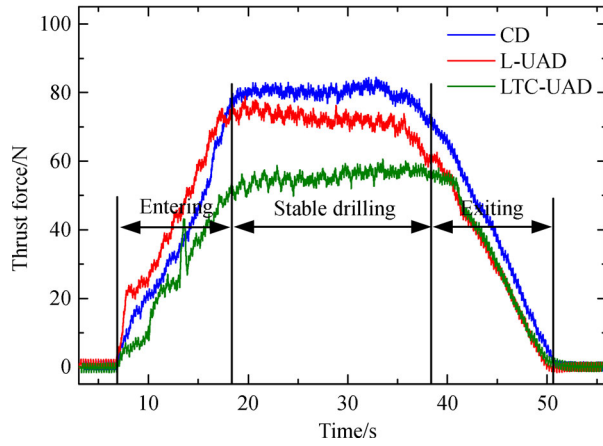| Spindle speed, n	Feed rate, F	Ultrasonic frequency, f	Longitudinal amplitude, A_L	Torsional amplitude, A_T
2000 r/min	0.005, 0.01, 0.015, and 0.02 mm/r	28.5 kHz	12 μm	4.8 μm

Fig. 7 Thrust forces vs. time for CD, L-UAD, and LTC-UAD (n = 2000 r/min, F = 0.005 mm/r).

gradually declines, so the thrust force drops rapidly. When the drill completely drills out the material, the thrust force becomes zero.

The maximum thrust force obtained from the measured data is taken as the final thrust force in each group of experiments. Figure 8 shows the variation trend of thrust force with time at different feed rates when the spindle speed is 2000 r/min. The modes of ultrasonic vibration can greatly affect the magnitude of the thrust force. The thrust forces under all three conditions show an increasing tendency with the feed rate. Given the existence of ultrasonic vibration, the thrust forces in L-UAD and LTC-UAD are distinctly lower than that in CD, and the maximum percentage of thrust force drop in LTC-UAD reaches 39% compared to that in CD. Many studies [12,17,18] have reported that L-UAD can significantly reduce the thrust force of drilling. Unlike L-UAD, the main cutting edge in LTC-UAD exerts a high-frequency intermittent impact on the hole bottom material in both
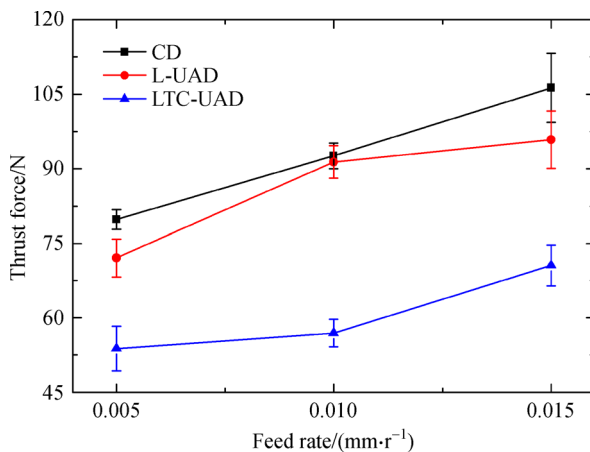
longitudinal and tangential directions. The removal of CFRP composites is mainly accomplished by the cutting action of the main cutting edge in the tangential direction, while the axial movement continuously feeds the drill. Therefore, the torsional vibration of the drill in the tangential direction is more conducive to the removal of the carbon fiber by shear fracture, and the shear strength of the carbon fiber is much lower than its tensile strength, decreasing the thrust force and improving the hole quality.

4.2 Delamination and burrs

With the feeding movement of the drill, the supporting stiffness of the uncut layers at the exit side gradually decreases. Therefore, the delamination defects near the hole exit are more prone to occur under the action of thrust force. Figure 9 depicts the effect of feed rate on the delamination factors (F_D) obtained when drilling CFRP composites in CD, L-UAD, and LTC-UAD. The delamination factors of the three drilling processes increase with the feed rate. Obviously, L-UAD and LTC-UAD contribute to reducing the value of F_D compared to CD, and LTC-UAD obtains the largest reduction in delamination factor F_D through suppressing the thrust force, which is consistent with the results of thrust forces recorded in Fig. 8. The small thrust force helps suppress the generation of delamination defects in CFRP composites.

The burr factor (F_B) was calculated at different feed rates for the holes drilled by CD, L-UAD, and LTC-UAD. As shown in Fig. 10, L-UAD and LTC-UAD induce less exit burrs than CD, and the burr factor calculated for LTC-UAD is lower than that for L-UAD at the same drilling parameters. The relationship between the feed rate and the burr factor is positively correlated under the three conditions because the increasing feed rate produces a larger thrust force, which results in larger burrs.
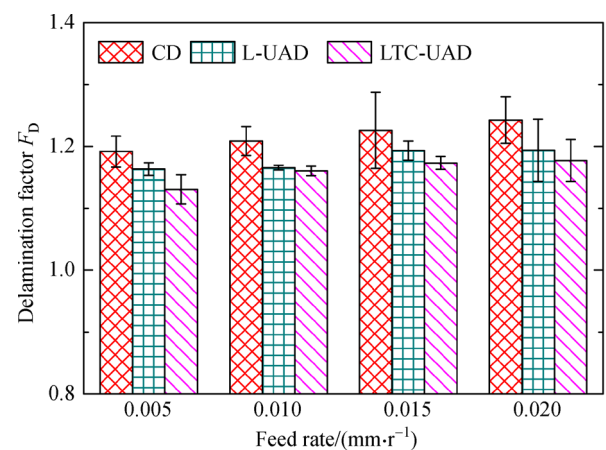

Fig. 8 Effect of feed rate on the thrust force in CD, L-UAD and LTC-UAD of CFRP.

Fig. 9 Effect of feed rate on the delamination factors of hole exit by CD, L-UAD, and LTC-UAD.

4.3 Surface roughness of the hole wall

The arithmetic mean deviation (Ra) parameter, which is widely applied in surface quality evaluation, was chosen to evaluate the surface roughness of hole wall in all experiments. All surface roughness values obtained after CD, L-UAD, and LTC-UAD at different feed rates are presented in Fig. 11. The surface roughness values of the hole wall drilled by L-UAD and LTC-UAD are much lower than those by CD, which is consistent with the results of other research [29]. Notably, LTC-UAD can produce a better hole wall quality with a lower surface roughness than L-UAD. The improvement of roughness can be explained by the polishing effect, which is generated by the multiple movements of the side edges of the drill, including the conventional drilling movement and the high-frequency longitudinal and torsional vibrations.

4.4 Hole surface morphology

Figure 12 shows the micro-morphologies of the hole wall drilled by CD, L-UAD, and LTC-UAD at 500× magni-

fication. Ultrasonic vibration modes have a significant influence on the micro-morphology of the drilled hole wall. In the absence of resin adhesion, the fibers that have been cut remain bare, resulting in the deterioration of the hole wall quality and many bare fibers on the hole wall in CD as shown in Fig. 12(a). Figure 12(b) shows the resin adhesion phenomenon on the hole wall in L-UAD and shallow cavities. As shown in Fig. 12(c), most areas of the hole wall in LTC-UAD are coated with resin, while only few cavities can be seen on the hole wall. Furthermore, unlike that of the hole wall in L-UAD and CD, the micro-morphology of the hole wall in LTC-UAD is relatively smooth. The obvious difference in the micro-morphology of hole wall above can be attributed to the fact that side edge of the drill in LTC-UAD is subjected to high-frequency longitudinal and torsional vibrations, which produce the repeated scraping effect of the side edge on the hole wall. Consequently, the resin is evenly coated on the hole wall, covering the cavities formed by fiber pulling and fiber/resin debonding. Therefore, the quality of the hole wall is relatively higher.

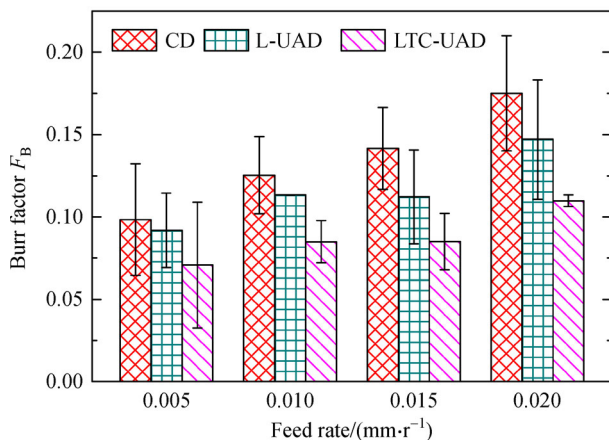Figure 13 presents the micro-morphology of the CFRP hole surfaces drilled by CD, L-UAD, and LTC-UAD at

Fig. 10 Effect of feed rate on the burr factors of hole exit by CD, L-UAD, and LTC-UAD.
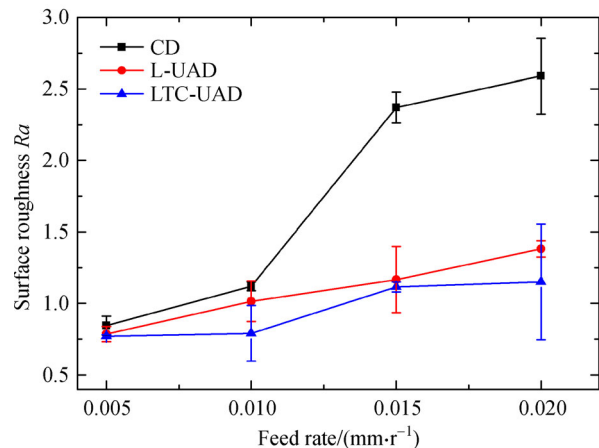

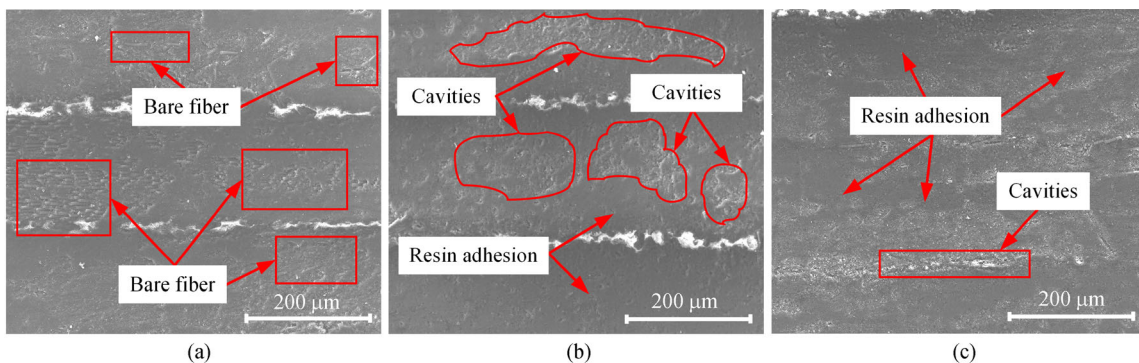**Fig. 11** Effect of feed rate on the surface roughness of the hole wall drilled by CD, L-UAD and LTC-UAD.

Fig. 12 SEM images of CFRP hole wall drilled by (a) CD, (b) L-UAD, (c) LTC-UAD ($n = 2000$ r/min, $F = 0.005$ mm/r, 500×).
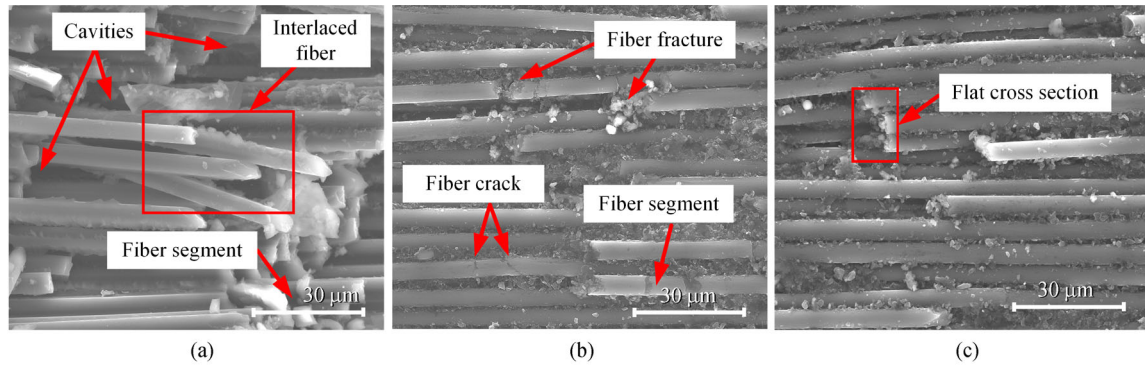
Fig. 13   SEM images of CFRP hole wall drilled by (a) CD, (b) L-UAD, (c) LTC-UAD ($n = 2000$ r/min, $F = 0.005$ mm/r, 3000×).

$3000×$ magnification. As shown in Fig. 13(a), some small cavities are formed on the hole wall under the large cutting force in CD with the removal of the material, and the fibers interlace each other under the action of the main cutting edge, producing a poor surface quality. Figure 13(b) shows fiber fracture, cracks, and segments on the hole wall in L-UAD, while the carbon fibers are partly surrounded by resin. Thus, L-UAD can obtain better hole quality than CD. Figure 13(c) indicates that a relative flat fracturing cross section of fiber can be obtained in LTC-UAD. The fibers on the hole wall are surrounded by resin and arranged evenly without fiber cracks and segments, indicating a hole wall with high quality.

5   Conclusions

In this work, drilling experiments were performed on CFRP composites using a self-developed LTC-UAD system and the L-UAD system to study their drilling performance in terms of thrust force, hole defects, hole wall roughness, and surface morphology. The main conclusions are as follows:

1) The kinematic equations of LTC-UAD were established by taking the actual rotating angle as the intermediate variable, and the kinematic characteristics of LTC-UAD were analyzed. LTC ultrasonic vibration produces the drill periodic variable motion in both axial and tangential directions, and the torsional vibration of the drill in the tangential direction is more conducive to the removal of the carbon fiber by shear fracture, which contributes to reducing the thrust force and improving the drilling quality of CFRP composites.

2) LTC-UAD and L-UAD contribute to the reduction of thrust force, and a significant reduction of thrust force by LTC-UAD (i.e., maximum of 39%) was obtained compared to that of CD because the LTC vibration of the cutting edge helps remove the carbon fiber through the shear fracture mode and change the contacting state between the cutting edge and the materials from continuous contact to discontinuous contact.

3) LTC-UAD can obtain lower delamination and burr factors and better surface quality of the hole wall than L-UAD and CD, indicating that LTC-UAD can effectively suppress the hole defects of the CFRP composites induced by drilling.

4) The holes drilled by LTC-UAD show high quality of the hole wall. Resin adhesion is conducive to improving the quality of the hole wall, and the torsional vibration of the side edge of the drill in LTC-UAD helps strengthen the effect of resin adhesion.

References

1. Chung D D L. Composite Materials: Science and Applications. 2nd ed. London: Springer, 2010, 30–32
2. Srivatsan T S. A review of: "*Fundamentals of Composites Manufacturing: Materials, Methods and Applications*" by A. Brent Strong. Materials and Manufacturing Processes, 1995, 10(5): 1121–1122
3. Davim J P, Reis P. Drilling carbon fiber reinforced plastics manufactured by autoclave-experimental and statistical study. Materials & Design, 2003, 24(5): 315–324
4. Singh A P, Sharma M, Singh I. A review of modeling and control during drilling of fiber reinforced plastic composites. Composites Part B, Engineering, 2013, 47: 118–125
5. Prabu V A, Kumaran S T, Uthayakumar M. Performance evaluation of abrasive water jet machining on banana fiber reinforced polyester composite. Journal of Natural Fibers, 2017, 14(3): 450–457
6. Hocheng H, Tsao C C. Effects of special drill tools on drilling-induced delamination of composite materials. International Journal of Machine Tools and Manufacture, 2006, 46(12–13): 1403–1416
7. Sorrentino L, Turchetta S, Bellini C. In process monitoring of cutting temperature during the drilling of FRP laminate. Composite Structures, 2017, 168: 549–561

8. Li C, Xu J Y, Chen M, et al. Tool wear processes in low frequency vibration assisted drilling of CFRP/Ti6Al4V stacks with forced air-cooling. Wear, 2019, 426–427: 1616–1623

9. Xu J, Mansori M E. Experimental studies on the cutting characteristics of hybrid CFRP/Ti stacks. Procedia Manufacturing, 2016, 5: 270–281

10. Liu D F, Tang Y J, Cong W L. A review of mechanical drilling for composite laminates. Composite Structures, 2012, 94(4): 1265–1279

11. Geng D X, Liu Y H, Shao Z Y, et al. Delamination formation, evaluation and suppression during drilling of composite laminates: A review. Composite Structures, 2019, 216: 168–186

12. Makhdum F, Jennings L T, Roy A, et al. Cutting forces in ultrasonically assisted drilling of carbon fiber reinforced plastics. Journal of Physics: Conference Series, 2012, 382: 012019

13. Lotfi M, Amini S. Experimental and numerical study of ultrasonically-assisted drilling. Ultrasonics, 2017, 75: 185–193

14. Debnath K, Singh I, Dvivedi A. Rotary mode ultrasonic drilling of glass fiber-reinforced epoxy laminates. Journal of Composite Materials, 2015, 49(8): 949–963

15. Phadnis V A, Makhdum F, Roy A, et al. Experimental and numerical investigations in conventional and ultrasonically assisted drilling of CFRP laminate. Procedia CIRP, 2012, 1: 455–459

16. Arul S, Vijayaraghavan L, Malhotra S K, et al. The effect of vibratory drilling on hole quality in polymeric composites. International Journal of Machine Tools and Manufacture, 2006, 46(3–4): 252–259

17. Makhdum F, Phadnis V A, Roy A, et al.. Effect of ultrasonically-assisted drilling on carbon-fiber-reinforced plastics. Journal of Sound and Vibration, 2014, 333(23): 5939–5952

18. Sanda A, Arriola I, Garcia Navas V, et al. Ultrasonically assisted drilling of carbon fiber reinforced plastics and Ti6Al4V. Journal of Manufacturing Processes, 2016, 22: 169–176

19. Xu W X, Zhang L C. On the mechanics and material removal mechanisms of vibration assisted cutting of unidirectional fiber-reinforced polymer composites. International Journal of Machine Tools and Manufacture, 2014, 80–81: 1–10

20. Geng D X, Zhang D Y, Li Z, et al. Feasibility study of ultrasonic elliptical vibration-assisted reaming of carbon fiber reinforced plastics/titanium alloy stacks. Ultrasonics, 2017, 75: 80–90

21. Liu J, Zhang D Y, Qin L G, et al. Feasibility study of the rotary ultrasonic elliptical machining of carbon fiber reinforced plastics (CFRP). International Journal of Machine Tools and Manufacture, 2012, 53(1): 141–150

22. Amini S, Soleimani M, Paktinat H. Effect of longitudinal-torsional vibration in ultrasonic-assisted drilling. Materials and Manufacturing Processes, 2017, 32(6): 616–622

23. Liu S, Shan X B, Cao W, et al. A longitudinal-torsional composite ultrasonic vibrator with thread grooves. Ceramics International, 2017, 43: S214–S220

24. Niu Y, Jiao F, Zhao B, et al. Multiobjective optimization of processing parameters in longitudinal-torsion ultrasonic assisted milling of Ti-6Al-4V. International Journal of Advanced Manufacturing Technology, 2017, 93(9–12): 4345–4356

25. Wang J J, Feng P F, Zhang J, et al. Reducing cutting force in rotary ultrasonic drilling of ceramic matrix composites with longitudinal-torsional coupled vibration. Manufacturing Letters, 2018, 18: 1–5

26. Paktinat H, Amini S. Numerical and experimental studies of longitudinal and longitudinal-torsional vibrations in drilling of AISI 1045. International Journal of Advanced Manufacturing Technology, 2018, 94: 2577–2592

27. Wang F J, Cheng D, Zhao M, et al. Influence of cooling air direction on tool wear and hole quality in CFRP drilling. Acta Materiae Compositae Sinica, 2019, 36(2): 410–417 (in Chinese)

28. Sadek A, Attia M H, Meshreki M, et al. Characterization and optimization of vibration-assisted drilling of fiber reinforced epoxy laminates. CIRP Annals-Manufacturing Technology, 2013, 62(1): 91–94

29. Thirumalai Kumaran S, Ko T J, Li C, et al. Rotary ultrasonic machining of woven CFRP composite in a cryogenic environment. Journal of Alloys and Compounds, 2017, 698: 984–993